jotaf Journal of Tekirdag Agricultural Faculty
Tekirdağ Ziraat Fakültesi Dergisi

Ocak/January 2026, 23(1)
Başvuru/Received: 27/11/24
Kabul/Accepted: 16/12/25
DOI: 10.33462/jotaf.1586666

'http://dergipark.gov.tr/jotaf
http://jotaf.nku.edu.tr/

ARAŞTIRMA MAKALESİ RESEARCH ARTICLE

Hyperspectral Imaging and Machine Learning for Assessing the Germination of Hydroprimed Lettuce Seeds*

Heiber Andres TRUJİLLO[1]*, Pedro Alexander VELASQUEZ-VASCONEZ[2], Rafael Mateus ALVES[3], Fernando Henrique IOST-FILHO[4], Francisco Guilhien GOMES-JUNIOR[5]

Abstract

Hyperspectral imaging (HSI) provides high-resolution spectral information across broad wavelength ranges and has emerged as a promising non-destructive approach for assessing seed quality. This study validated the use of HSI combined with machine learning to identify spectral features associated with germination performance in hydroprimed lettuce seeds. Seeds of the Roxa and Vanda genotypes were subjected to hydropriming, dried, and stored prior to evaluation. Hyperspectral images were acquired using 300 spectral bands spanning 384.7–1020.7 nm for each treatment, and mean spectra were used as predictors in classification models. Machine learning analysis was performed primarily with Random Forest to discriminate seed performance categories, including normal seedlings, abnormal seedlings, non-germinated seeds, and dead seeds. Feature-importance results indicated that wavelengths near 390 nm were among the most informative predictors of germination performance, whereas bands at 473–475 nm contributed comparatively less. The Random Forest models showed high sensitivity and specificity across the defined classes, supporting the feasibility of spectral-based categorization of seed outcomes. In complementary analyses, Ridge regression reinforced the relevance of peripheral regions of the spectrum, highlighting 384.73 nm and 874.57 nm as important for classification and underscoring the value of targeted band selection to improve model interpretability and efficiency. Hydropriming affected both spectral signatures and physiological responses, with genotype- and lot-dependent outcomes. In Roxa, selected seed lots exhibited superior performance in germination and vigor tests after hydropriming and storage. In Vanda, specific lots displayed greater uniformity and improved emergence indices. Overall, the integration of HSI and machine learning captured strong associations between spectral data and seed performance metrics, with high canonical correlations (R^2 = 0.91–0.99). These results demonstrate that HSI coupled with predictive modeling is an effective, rapid, and non-destructive strategy to assess the physiological quality of hydroprimed lettuce seeds and to support decision-making in seed lot classification.

Keywords: Computer vision, Image analysis, Seed germination, Electromagnetic spectrum, Random forest model

[1]***Sorumlu Yazar/Corresponding Author:** Heiber Andres Trujillo, Department of Crop Science, University of São Paulo, 'Luiz de Queiroz` College of Agriculture, 11 Pádua Dias Avenue, 13418-900, Piracicaba, SP, Brazil. E-mail: heiberandrestrujillo@gmail.com OrcID: 0000-0001-6604-9438
[2]Pedro Alexander Velasquez Vasconez, Basic Sciences, Technology, and Engineering College, National Open and Distance University, Pasto, Nariño, Colombia. E-mail: pedro.velasques@unad.edu.co OrcID: 0000-0002-7564-4519
[3]Rafael Mateus Alves, Department of Crop Science, University of São Paulo, 'Luiz de Queiroz` College of Agriculture, 11 Pádua Dias Avenue, 13418-900, Piracicaba, SP, Brazil. E-mail: rafaelalvesmateus@gmail.com OrcID: 0000-0003-3482-1010
[4]Fernando Henrique Iost Filho, Department of Entomology, University of São Paulo, 'Luiz de Queiroz` College of Agriculture, 11 Pádua Dias Avenue, 13418-900, Piracicaba, SP, Brazil. E-mail: fernandohiost@usp.br OrcID: 0000-0002-9116-5104
[5]Francisco Guilhien Gomes-Junior, Department of Crop Science, University of São Paulo, 'Luiz de Queiroz` College of Agriculture, 11 Pádua Dias Avenue, 13418-900, Piracicaba, SP, Brazil. E-mail: francisco1@usp.br OrcID: 0000-0001-9620-6270
Atıf/ Citation: Trujillo H. A., Velasquez-Vasconez P. A., Alves R. M., Iost-Filho F. H., Gomes-Junior F.G. (2026). Hyperspectral imaging and machine learning for assessing the germination of hydroprimed lettuce seeds. *Journal of Tekirdag Agricultural Faculty,* 23(1): 86-100.

*This study was summarized from the Heiber Andres Trujillo PhD thesis.

1. Introduction

Lettuce stands out as a nutritionally significant food and an economically important vegetable consumed globally. Seed value has increased substantially, making it a key criterion for selecting improved genotypes. Likewise, optimizing seed germination techniques and obtaining seedlings play a crucial role in lettuce production programs.

Hyperspectral imaging refers to capturing information about the intensity of light reflected or emitted by objects in different narrow and continuous bands of the electromagnetic spectrum (Wu and Sun, 2013). This technique enables the collection of data in hundreds or even thousands of spectral bands, enabling the identification of subtle patterns imperceptible in other forms of imaging (Dale et al., 2013). Hyperspectral images have been used to evaluate and monitor seed quality, detect diseases, identify deterioration patterns, and optimize seed production and selection processes (Feng et al., 2017). Studies in this field focus on identifying quality patterns based on image characteristics, including genotype classification (Feng et al., 2017; Ge et al., 2024; Sun et al., 2016; Wang et al., 2021; Xia et al., 2019), determination of moisture content (Yin et al., 2023), identification of damage and injuries (Wang et al., 2021), and detection of germination failures (Arngren et al., 2011; Guo et al., 2017; Singh et al., 2009; Xing et al., 2010). Another application of hyperspectral imaging in seeds is the assessment of vigor. In this context, hyperspectral imaging has proven useful for analyzing seeds from various vegetable species and for identifying spectral patterns associated with viability (Zhang et al., 2014), thereby supporting the production of high-quality seedlings (Feng et al., 2017; Liu et al., 2016). The implementation of hyperspectral analysis, together with machine learning techniques, especially predictive algorithms, has received attention in current research in the seed sector (Cheng et al., 2023; Qiu et al., 2023; Zhao et al., 2018; Zou et al., 2022). However, one of the critical steps in processing hyperspectral image data is selecting the useful bands within the electromagnetic spectrum, which can provide valuable information about the physiological state of the seeds.

Seed hydropriming is a widely adopted pre-germination treatment to improve seed quality and germination potential. Hydropriming involves the controlled hydration of seeds so that they absorb water and undergo the first stage of germination without the occurrence of primary root protrusion (Ali et al., 1990; Ibrahim, 2016; Raj and Raj, 2019). This technique aims to prepare the seeds for germination by activating essential metabolic processes, followed by drying them to reach the initial water content of the sample (Farooq et al., 2006). The application of seed hydropriming significantly enhances the speed and uniformity of germination (Bruggink et al., 1999) while also promoting resistance to abiotic factors that affect seedling emergence (Beyaz, 2023). In crops like lettuce, which have variable germination potential and seedling emergence, hydropriming can be a promising technique to standardize and enhance the physiological performance of seeds.

The integration of hyperspectral imaging with machine learning algorithms allows the identification of specific spectral bands that are most relevant to germination performance, enabling precise and non-destructive seed quality assessment, while the application of Random Forest and SMOTE contributes to improved classification performance in unbalanced datasets. The objective of this research was to validate the utility of hyperspectral images and machine learning algorithms based on Random Forest in determining wavelength parameters associated with the germination performance of hydroprimed lettuce seeds.

2. Materials and Methods

The research was conducted at the Image Analysis and Seed Analysis Laboratories of the Department of Crop Science and the Integrated Pest Management Laboratory of the Department of Entomology and Acarology at the 'Luiz de Queiroz' College of Agriculture, University of São Paulo, in Piracicaba, SP, Brazil.

2.1. Seed Hydropriming

Lettuce (*Lactuca sativa)* seeds from the genotypes Scarlet Red Curly (Scarlet) and Vanda Curly (Vanda) were used, provided by Sakata Seed Sudamerica Ltd. Each genotype was represented by five seed lots with germination within commercial standards and varying levels of vigor. Each seed lot was divided into four samples: i) unprimed seeds (control), ii) wet hydroprimed seeds (post-hydropriming), iii) dried hydroprimed seeds (dried in an oven at 30°C and 45-55% relative humidity for 96 hours), and iv) hydroprimed seeds, dried and stored in a cold, dry chamber at 10°C and 30% relative humidity for three months.

Hydropriming was performed using the drum method. First, the water imbibition curve was determined with four replicates of 1 gram of seeds, with data expressed as the percentage of water content of each lot (Alves et al., 2023). The amount of water was administered using the HIDRO-Control® device, consisting of a rotating acrylic drum, a synchronous motor, a water tank, an electric pump, and two timers (Figure 1A). Water application was done at one-hour intervals until reaching the total volume required for each lot (Kikuti and Marcos Filho, 2012).

2.2. Hyperspectral İmage Analysis of Seeds

For obtaining the hyperspectral images, a Pushbroom hyperspectral scanning camera (PIKA L, Resonon Inc., Bozeman, MT, USA) equipped with a 23 mm objective lens was employed (*Figure 1*). The camera sensor captures spectral data in the range of 384.73 to 1020.76 nm (spectral range), comprising 300 bands (spectral channels) with a spectral resolution of 3 nm and a spectral bandwidth of 2.1 nm, with 900 spatial pixels per line. For spectral data collection, eight replicates of 25 seeds from each treatment were placed on acetate slides and positioned on a linear platform under the sensor, at a distance of 30 cm from the camera. This platform moves automatically, acquiring data controlled by the Spectronon software (Resonon Inc., Bozeman, MT, USA). Hyperspectral images were acquired in a dark room environment, artificially illuminated by a tower mounted with 15W, 12V LED lamps arranged in two inclined rows, one on each side of the lens (*Figure 1B*). A polyethylene plastic plate (Type 822, Spectronon Pro Resonon, Bozeman, MT, USA) was used for white calibration, while the lens cap was used for dark calibration (Alves et al., 2023; Iost Filho et al., 2022). The spectral data from the images were manually extracted from each data cube corresponding to the spectral sample of each seed. These data represent the average reflectance value of the area of interest (total seed area) for each of the 300 bands, covering wavelengths between 384.73 and 1021.76 nm (*Figure 1C*).

2.3. Germination Performance Evaluation Framework

After acquiring the spectral values of the seeds in each treatment, seed germination performance was determined using the germination test and moisture content (Brasil, 2009), seedling emergence, accelerated aging in saturated NaCl solution (Kikuti and Marcos Filho, 2012), and vigor calculation using the Seed Vigor Image System (SVIS®) (Sako et al., 2001) (*Figure 1D*).

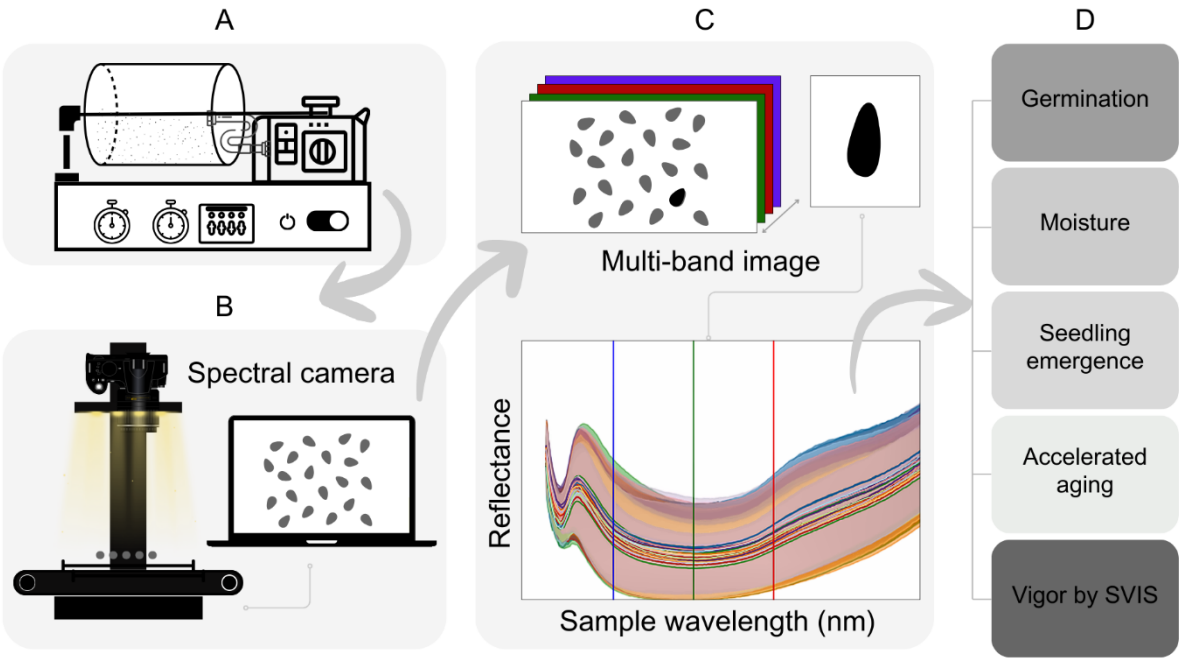

Figure 1. Acquisition and hyperspectral image analysis flow of lettuce seeds. Steps include drum hydropriming method (A), image acquisition by Pushbroom hyperspectral camera (B), selection, segmentation of the seed spectral sample, and obtaining the average spectrum of the sample selection using Spectronon software (C), and seed germination performance (D)

2.4. Statistical Analysis

ANOVA was used to study differences in hyperspectral bands based on genotype and seed treatment (unprimed, wet hydroprimed, dry hydroprimed, and stored hydroprimed). The experiment was set up as a randomized complete block design (blocks) with two factors: the first factor corresponding to genotype (2 levels), and the second factor corresponding to seed treatment (4 levels). Subsequently, MANOVA was conducted to assess how treatments influenced seed hyperspectral properties. Different statistical criteria such as Pillai, Hotelling-Lawley, Wilks, and Roy were used to determine the significance of treatments considering all response variables (Xu et al., 2022; Cheng et al., 2023).

To assess the predictive capability of spectral variables on seed germination, the general Random Forest model (Equation 1) and the Synthetic Minority Over-sampling Technique (SMOTE) were used. Random Forest is a supervised learning algorithm based on decision trees, where each tree in the forest is trained with random subsets of the data. The final prediction is based on the average or majority vote of the trees. SMOTE was used to address the class imbalance in the dataset by generating synthetic samples to increase the representation of minority classes. This improved the robustness and performance of the Random Forest model, particularly in terms of specificity and classification balance for underrepresented classes.

Data were divided into training and test sets, 70% and 30% respectively, using the rf_model.fit(X_train, y_train) algorithm. Random Forest was built with 500 trees and evaluated through 5-fold cross-validation, focusing on the germination variable. After training, the model was tested for predictions, and its performance was evaluated using various metrics, including accuracy, specificity, precision, recall, F1-score, area under the curve (AUC), and variable importance based on the Mean Decrease Gini criterion. These metrics were used to assess both the overall model performance and its discriminative capacity. AUC analysis was conducted for each germination class (normal seedling, abnormal seedling, non-germinated seed, and dead seed — seeds with microorganisms). Overall metrics, such as total accuracy, Kappa index, and global AUC, were also considered for a summarized assessment of model performance across the entire test dataset (Huang et al., 2016).

The evaluation metrics used to assess the performance of machine learning models include: (i) accuracy, which measures the overall proportion of correctly classified instances; (ii) precision, the proportion of true positives among all predicted positives; (iii) recall (or sensitivity), the proportion of true positives among all actual positives; (iv) F1-score, the harmonic mean of precision and recall, useful in imbalanced datasets; (v) specificity, which indicates the true negative rate; (vi) AUC (Area Under the Curve), reflecting the ability of the model to distinguish between classes; and (vii) Kappa index, which adjusts accuracy for the agreement expected by chance.

$$H(x) = \arg \max_{c\epsilon\{1,\dots,C\}} \sum_{k=1}^{K} I\left(h_k(X) = C\right) \quad \text{(Eq. 1).}$$

I is the indicator function that equals 1 when $hk\ (x)$ = C and 0 otherwise.

The importance of each spectrum as an independent variable was determined using the Random Forest importance function based on the Mean Decrease Gini criterion. Additionally, a Ridge Regularization Multinomial Regression Analysis was conducted to quantify the importance of spectral variables based on model coefficients. Ridge regularization was adjusted using the cv.glmnet function from the glmnet package in R software.

To determine the linear relationship between hyperspectral image analysis methodology and germination performance along with vigor parameters by SVIS®, a Canonical Correlation Multivariate Analysis was conducted. This analysis considered two groups of metric variables, identified as dependent variables (spectral values) and others as independent variables (germination performance tests and vigor). However, in the latter group, the wet hydroprimed seed treatment was not included as the seeds used in this treatment were the same as those in the dry hydroprimed seed treatment. Statistical procedures were made in the R language (R Core Team, 2023) (Christensen, 2023).

3. Results and Discussion

3.1. Effects of Hydropriming on Hyperspectral Bands and Germination Predictions

Hydropriming notably impacts the hyperspectral attributes of lettuce seeds. Hydropriming treatment had a significant influence ($p < 0.01$) on spectral bands. Differences in spectral bands were observed between the Roxa

and Vanda genotypes, along with corresponding wavelength values at bands 388.74 and 1005.98 nm, representing the lower and upper extremes of the spectral curve (*Figure 2*). Additionally, analysis of variance (ANOVA) revealed that each genotype possesses a distinct spectral signature. Seed lots showed no significant effect, indicating high homogeneity among them, which is sufficient not to influence the hyperspectral characteristics of the images. Furthermore, the results highlighted significant effects ($p < 0.01$) in the interaction between genotypes and seed treatments, i.e., Roxa or Vanda seeds × unprimed, wet hydroprimed, dry hydroprimed, and hydroprimed stored seeds, confirming that the response to hydropriming varies exclusively by genotype. Multivariate analysis of variance (MANOVA) provided additional results demonstrating the significance of treatment effects on the hyperspectral properties of seeds, with notable differences in response by genotype. The test results confirmed the conclusions drawn from individual band ANOVA, showing similar significances for each factor and their interactions. Thus, the analysis conducted based on multiple tests (Pillai, Hotelling-Lawley, Wilks, and Roy) confirmed the significant effect of hydropriming on the set of hyperspectral bands, affecting Roxa and Vanda differently.

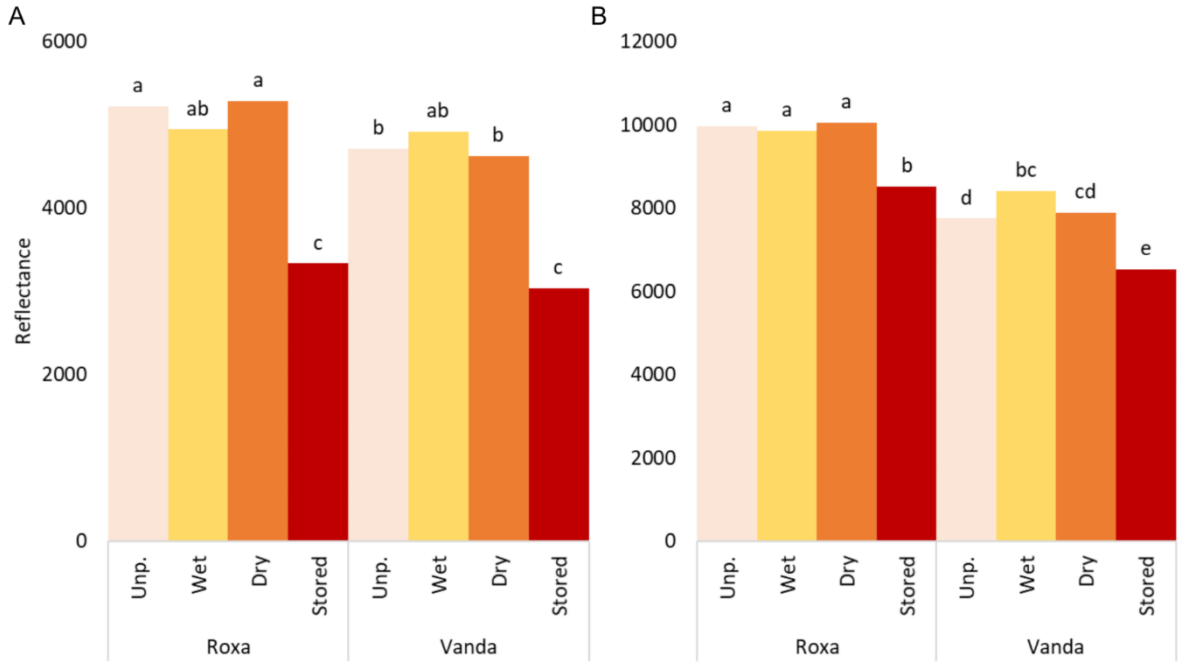

Figure 2. Reflectance values at spectral bands 388.74 nm (A) and 1005.98 nm (B) of lettuce seeds due to hydropriming

The analysis using Random Forest showed bands in the range of 384, 390, 386, and 388 nm to be the most relevant in predicting the physiological germination characteristics of the seeds. Conversely, the least important bands were found in the range of 473, 483, 471, 475, and 467 nm, respectively (Figure 3). These results highlight the relative importance of each band in the Random Forest and SMOTE algorithm predictions for hyperspectral seed images. Specifically, the most prominent bands included those with higher importance values, such as bands at 386, 384, 392, and 390 nm, respectively. Bands with lower importance were identified at wavelengths like 954, 512, 793, and 804 nm (*Figure 3*). The significance of these features indicates their crucial role in the algorithm's ability to predict seed performance, even prior to germination, demonstrating an efficient non-destructive method in high-throughput phenotyping, particularly in determining spectral wavelengths of seeds related to germination (further).

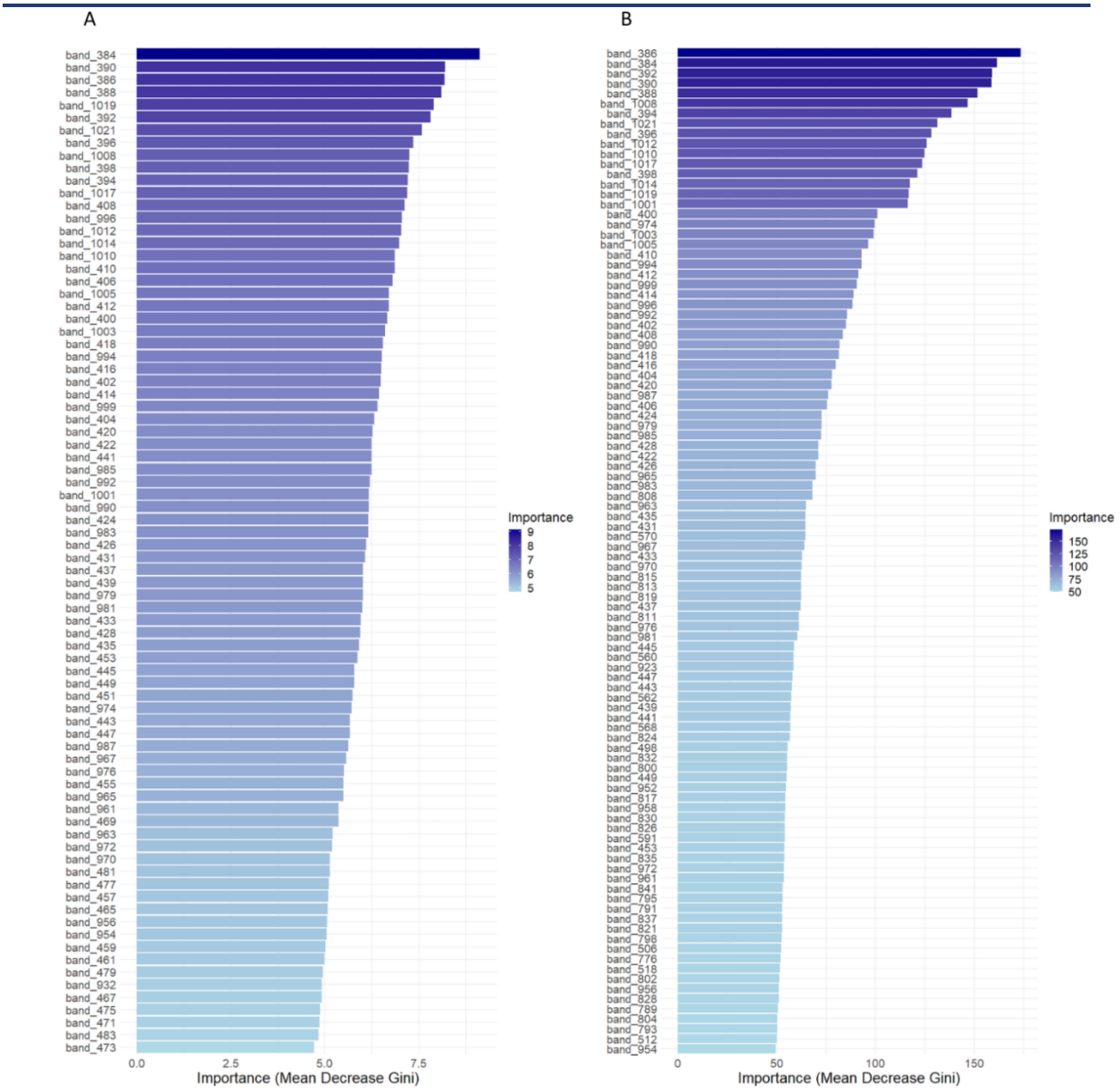

Figure 3. Feature importance Random Forest (A) and Random Forest SMOTE (B) variables, measured by the Gini Decrease Index, using spectral values of lettuce seeds subjected to hydropriming

With respect to the spectral characteristics of the seeds and the results of their germination test, the Random Forest algorithm demonstrated high specificity for abnormal seedlings, non-germinated seeds, and dead seeds, with values close to 1, highlighting its ability to correctly identify these categories. However, there was a discrepancy in specificity for normal seedlings, showing less effectiveness in this parameter. On the other hand, the precision for this same classification reached values of 0.87, the highest observed. The algorithm's accuracy was moderate in all cases. Additionally, the algorithm exhibited high sensitivity and balance in the classification of normal seedlings. When applying Random Forest SMOTE, a significant improvement in specificity for normal seedlings was observed, along with increased precision, sensitivity, and balance for non-germinated seeds, abnormal seedlings, and dead seeds (*Figure 4*). These improvements resulted in a more robust and reliable algorithm, capable of handling unbalanced datasets more efficiently in this classification. Finally, the area under the curve (AUC) was also moderate in all cases, indicating solid overall performance of the SMOTE-enhanced Random Forest algorithm. Overall, the results indicate that Random Forest SMOTE is suitable for high-performance phenotyping techniques based on seed germination through hyperspectral image analysis.

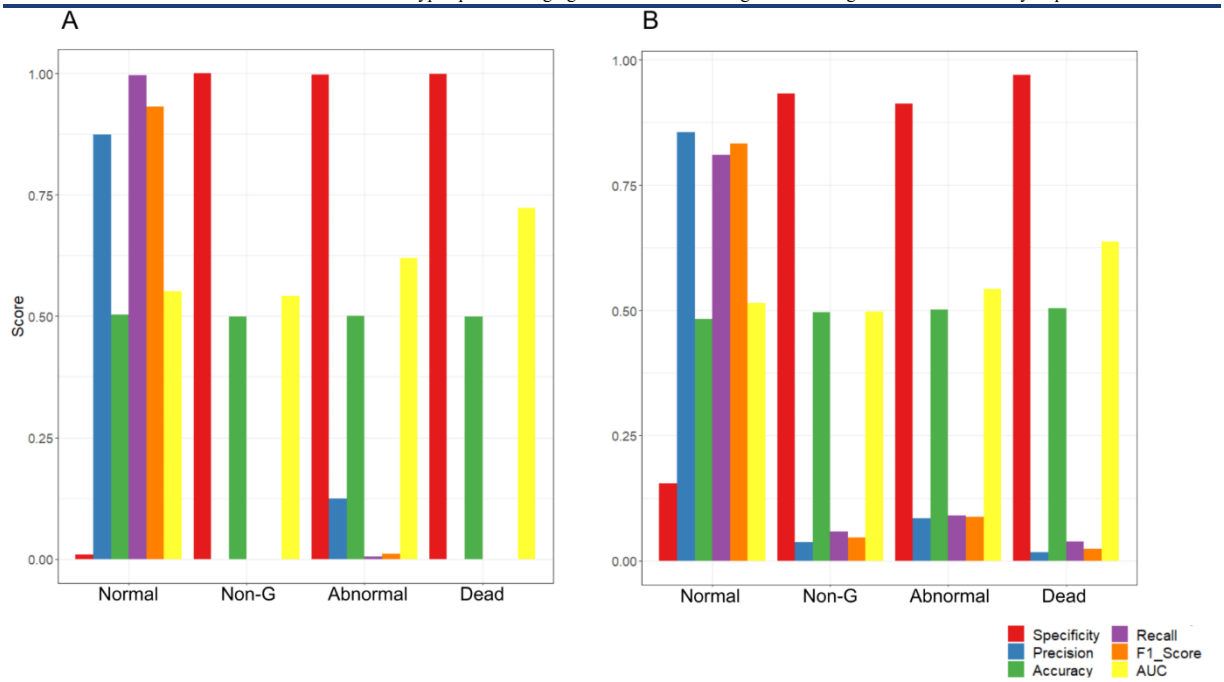

Figure 4. Metrics of Random Forest (A) and Random Forest SMOTE (B) for predicting germination in lettuce seeds after hydropriming, using spectral values from seed images

The treatments applied to the seeds caused a more pronounced impact on the spectral edges. When employing Ridge Regression to estimate seed conditions based on treatment, it was evident that the spectral edge bands may have greater relevance in developing predictive algorithms. It was observed that at least 28 important bands out of the 300 spectral bands obtained from the images had coefficients greater than |0.1|, with seven of the edge bands having the highest weights. The regression coefficients (associated with the independent variables of the algorithm) ranged from -4 to 6, with bands 384.73 nm (ultraviolet, UV-C region) and 874.57 nm standing out as those showing the most substantial weights (Figure 5). Interestingly, despite the high relevance observed, the 874.57 nm band was not identified as the most significant based on variable importance measures derived from mean decrease in Gini index, which pointed to greater importance for the 386.73 nm band (Figure 5). These results indicate that depending on the algorithm used, specific bands may need to be selected that better fit the dataset.

The analysis of sensitivity and specificity at different classification thresholds during lettuce seed germination revealed significant results. Both ROC Random Forest and ROC Random Forest SMOTE demonstrated efficient discrimination of normal, abnormal seedlings, and non-germinated seeds. However, the algorithm exhibited superior performance in discriminating dead seeds, establishing a direct relationship between the classification of spectral bands from seed images and this category in the germination test (Figure 6). The ROC curve approaching the upper left corner of the graph indicates high sensitivity and specificity of the applied algorithm compared to a random algorithm. Based on accuracy values in both cases, it can be considered that the algorithm is suitable for correctly predicting seed classes based on spectral signatures from seed images. The AUC measure, which assesses the algorithm's ability to distinguish between positive and negative classes, showed acceptable performance in classifying the classes. Additionally, the Kappa coefficient, which evaluates the agreement between algorithm predictions and actual observations, considering the agreement that could be expected by chance alone, indicated stronger agreement between algorithm predictions and real data (*Figure 6*).

The bands with higher importance significantly contributed to the algorithm's performance in classifying or predicting seed characteristics from hyperspectral images. These specific bands could potentially be valuable in genetic improvement programs aimed at identifying seeds with better physiological potential and early seedling stages, allowing screening of a large population of plants at lower cost and without damaging seedlings. Similarly, they may be more sensitive to seed biochemistry influenced by different treatments, which could be valuable for implementing classification techniques based on image use without sample damage, features widely desired and previously used in these methodologies (Alves et al., 2023; Zhang et al., 2020). In contrast to other researches that applied Principal Component Analysis (PCA) and did not consider spectral extremes in determining the most

relevant bands in hyperspectral analysis for seed classification algorithms (Alves et al., 2023; Bai et al., 2024; Iost Filho et al., 2022), this method was not applied. This decision stemmed from PCA being considered an intermediate method, optionally used for regression techniques, factor analysis, clustering analysis, or predictive methods including Random Forest. The results also suggest that the spectral extremes analyzed can be widely influenced by the seed treatment process, indicating a potential area for seed classification based on non-destructive attributes and statistical efficiency.

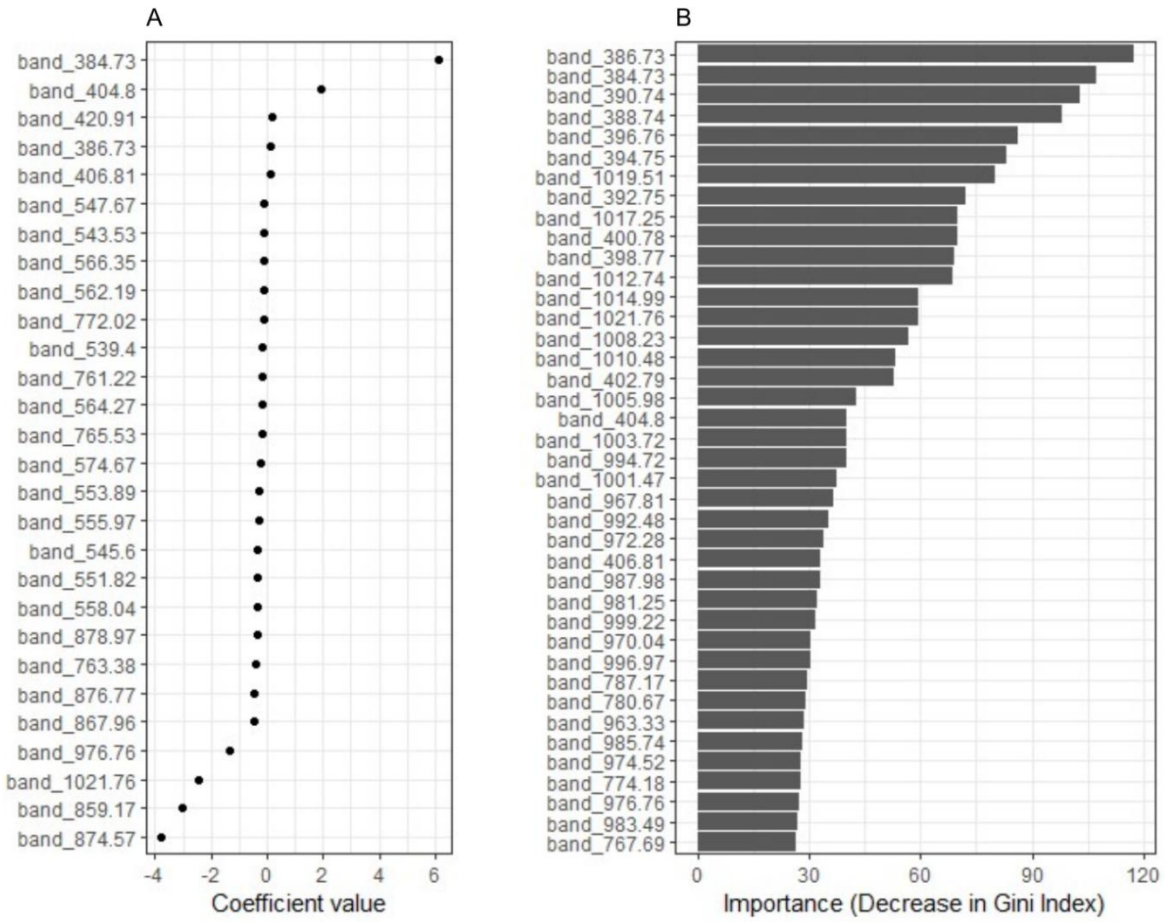

Figure 5. Analysis of coefficients in Ridge Regression (A) and evaluation of variable importance in the algorithm using the Gini Decrease Index (B), using spectral values of lettuce seeds subjected to hydropriming

The predictive metrics were compelling and indicate potential applicability of spectra when analyzed with machine learning algorithms. To our knowledge, this is the first algorithm for early selection of lettuce seeds using this technology, although promising results exist for other species. Different preprocessing methods and machine learning techniques offer significant advantages in identifying seed vigor and can effectively improve accuracy and efficiency (Xu et al., 2022). The algorithm combining preprocessing, wavelength selection, and machine learning showed promising results in classifying seeds of different species. According to Xu et al., 2022, the DE-UVE-ANN algorithm achieved the best discrimination results, with a prediction accuracy of 95.24% for maize seed viability. Using performance metrics from the MLP-ANN prediction algorithm (Iost Filho et al., 2022), overall accuracy ranged from 72% to 73%. In contrast, the Kappa coefficient and other algorithm-related metrics (Precision and Recall) also reached values of 0.70 in the test set for soybean plants under abiotic stress. For the proposed analysis in lettuce seed quality classification, predictive power metrics are likely to be enhanced by including new observations or adding more seed parameters that have not yet been considered. For example, seed weight, seedling size, and other attributes in the early growth stages of plants could be used in seed classification. Parameters such as yield, vegetation indices, and plant size showed high correlation, measured by Spearman correlation, with the wavelengths analyzed by the Random Forest algorithm in classifying soybean genotypes in different environments (Parmley et al., 2019). However, the mentioned characteristics demonstrate the effectiveness and reliability of the algorithm in classifying different seed classes based on spectral information

from images. These findings confirm the applicability and utility of the Random Forest and SMOTE algorithm in this specific context.

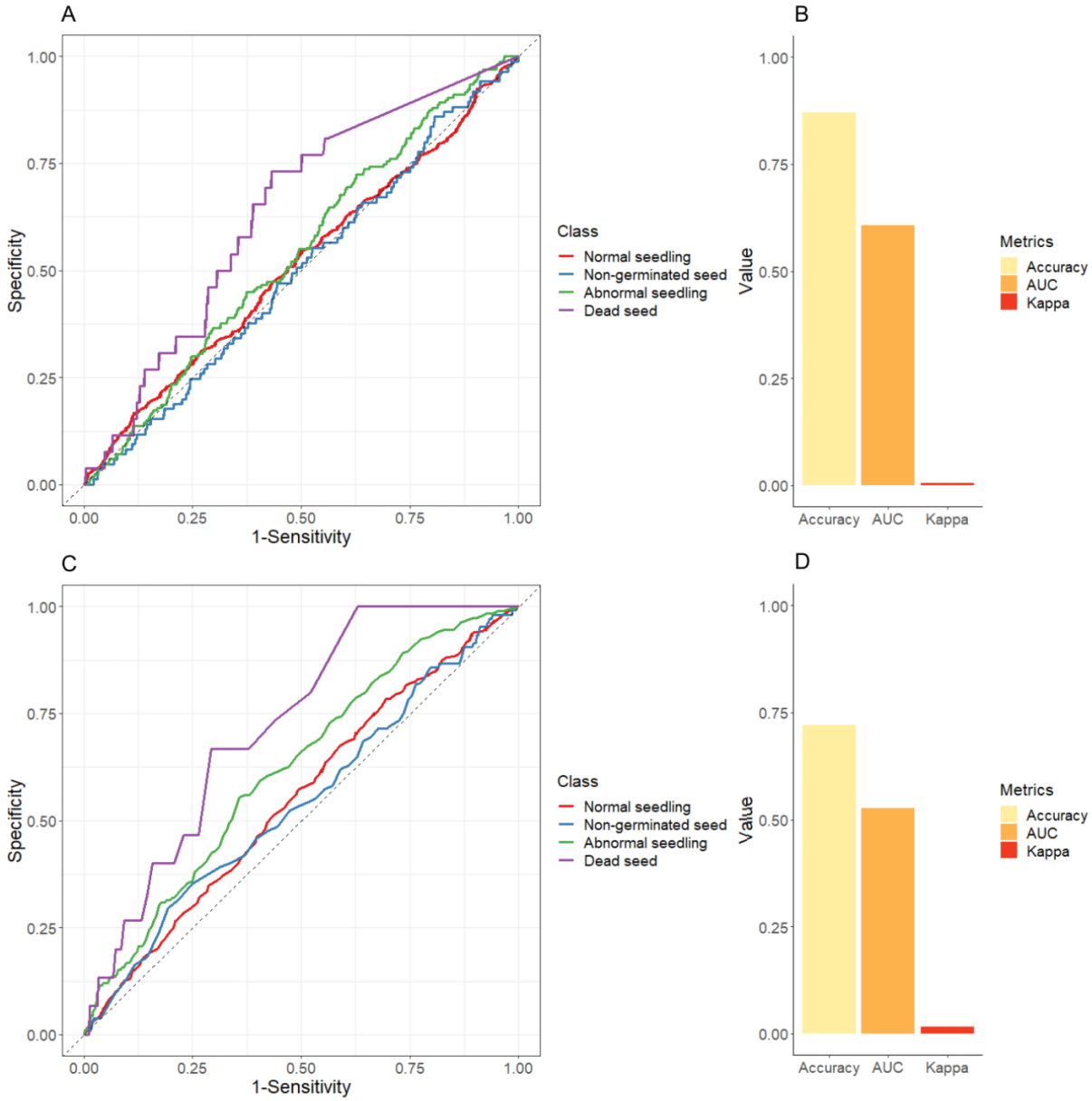

Figure 6. ROC curves of Random Forest SMOTE (A) and performance metrics (Accuracy, AUC, Kappa) (B), ROC curves of Random Forest (C) and performance metrics (Accuracy, AUC, Kappa) (D), using spectral values from lettuce seeds subjected to hydropriming

Although the main groups of bands providing information on the influence of hydropriming on the spectral characteristics of lettuce seeds have been identified, variations in spectral scale values may be influenced by various factors, including the biochemical composition of the seeds. Previous research highlights the relationship between different spectral bands and biochemical content. Spectral bands at 1449.28 nm are primarily related to water content (Krepper et al., 2018; Xu et al., 2022). In the range of 1100 to 1250 nm, bands are related to the overtones of CH stretching modes of CH3 and CH2 groups, as well as their combinations (Choi et al., 2020). Spectra located in the regions of 1200 and 1300 to 1400 nm are associated with the presence of carbohydrates (Alhamdan and Atia, 2017; Yin et al., 2017). Protein content is associated with bands 1208, 1420, 1430, 1450, 1465, and 1550 nm (Loewe et al., 2017; Yin et al., 2017). Differences in reflectance of bands between 1399 to 1699 nm have been linked to C-H and O-H bonds, also related to water activity and phenolics (Nicolaï et al., 2007). The wavelength region of 1700 to 1710 nm is related to C-H bonds (particularly CH3), relevant to organic materials such as fatty acids (Choi et al., 2020). Seed viability is not limited to the reflectance in the spectral image but is

intrinsically linked to the integrity of the seeds themselves (Zhang et al., 2020). Therefore, bio-chemical analysis would be appropriate to correlate and explain the variation in wavelengths and their changes during different phases of hydropriming treatment of lettuce seeds.

3.2. Performance of Hydroconditioned Seeds and Machine Learning Models

When seeds subjected to hydropriming were evaluated using hyperspectral analysis, germination, and vigor tests, different levels of vigor were revealed for both the Roxa and Vanda genotypes (*Tables* 1 and *2*). The moisture content varied in both cases. However, for the treatments, the unprimed seeds of the Roxa genotype, which had higher moisture content (lot 7), also demonstrated a higher vigor index compared to lots 2, 6, and 8, and greater average seedling length compared to the other lots as indicated by SVIS® (*Table 1*). In the Roxa genotype, lots 2 and 4 among the unprimed seeds exhibited superior performance in the germination and first germination count tests. For dry hydroprimed seeds, lots 2 and 7 showed superior performance in germination, emergence, and seedling emergence rate index tests compared to the other studied lots. After hydropriming, drying, and subsequent storage, lot 2 continued to show superior performance in emergence, seedling emergence rate index, and seedling uniformity tests compared to the other lots. There was a notable reduction in the ability of seeds from lot 8 to maintain germination and seedling production after hydration and the storage period (*Table 1*).

Table 1. Quality parameters of lettuce seeds from the Roxa genotype, including moisture content (MC), first germination count (FGC), germination (G), germination after accelerated aging with NaCl saturated solution (AA), seedling emergence (SE), seedling emergence rate index (SEI), vigor index (VI), uniformity index (UI), and average seedling length (Length) obtained by SVIS® for unprimed, dry hydroprimed, and hydroprimed stored seeds

Roxa									
Lot	MC	FGC	G	AA	SE	SEI	VI	UI	Length
	..... %					..... Index			cm
Unprimed									
2	5.85	98 a	98 a	98 a	96 a	16 a	764 bc	785 a	3.54 b
4	6.25	95 ab	95 ab	94 abc	93 ab	16 a	788 ab	785 a	3.56 b
6	4.9	89 c	89 c	96 ab	88 b	14 b	697 c	781 a	3.01 c
7	7.15	91 bc	91 bc	91 bc	93 ab	15 ab	851 a	780 a	4.13 a
8	5.15	93 bc	93 bc	89 c	90 ab	15 ab	763bc	746 a	3.52 b
CV	.	3.3	3.3	3.65	4.28	5.08	10.6	5.91	13.47
Dry hydroprimed									
2	5.57	96 a	96 a	90 a	99 a	17 a	706 b	764 ab	3.11 b
4	6.35	91 a	94 ab	67 b	95 b	14 b	721 ab	763 ab	3.24 b
6	6.33	91 a	91 b	76 b	89 c	14 b	719 b	756 ab	3.29 b
7	7.1	94 a	95 ab	73 b	96 ab	16 a	790 a	779 a	3.66 a
8	6.13	91 a	91 b	66 b	91 c	15 b	675 b	715 b	2.99 b
CV	.	4.73	2.91	9.45	2.57	4.63	9.46	7.27	10.44
Hydroprimed stored									
2	3.5	97 a	97 a	58 a	100 a	16 a	841 a	822 a	3.84 a
4	6.22	92 ab	92 ab	38 b	87 b	13 b	746 b	747 b	3.41 b
6	5.7	84 c	84 c	61 a	82 b	13 b	743 b	684 c	3.4 b
7	4.67	93 ab	93 ab	44 b	90 b	14b	843 a	774 b	3.85 a
8	5.59	92 b	92 b	23 c	87 b	13 b	774 b	753 b	3.51 b
CV	.	3.67	3.67	14.74	6.09	6.83	9.46	7.27	10.44

Means sharing the same letter do not differ significantly according to the LSD test ($p \leq 0.05$)

In the case of the Vanda genotype, lots 4 and 5 demonstrated the best performance among the unprimed seeds in the first germination count, germination, and accelerated aging tests compared to the other lots (*Table 2*). Lot 4 showed better vigor index, uniformity, and average seedling length compared to lots 7, 8, and 9. Lot 5 showed superior performance in the emergence tests and seedling emergence rate index compared to lots 7, 8, and 9 (*Table 2*). After the hydropriming and drying process, lot 5 showed a difference compared to lots 7, 8, and 9 in terms of

emergence, seedling emergence rate index, vigor, uniformity, and average seedling length tests. After hydropriming and storage, lots 4 and 5 presented superior results in germination and first germination count tests (*Table 2*).

Table 2. Quality parameters of lettuce seeds from the Vanda genotype, including moisture content (MC), first germination count (FGC), germination (G), germination after accelerated aging with NaCl saturated solution (AA), seedling emergence (SE), seedling emergence rate index (SEI), vigor index (VI), uniformity index (UI), and average seedling length (Length) obtained by SVIS® for unprimed, dry hydroprimed, and hydroprimed stored seeds

Vanda									
Lot	MC	FGC	G	AA	SE	SEI	VI	UI	Length
	..... %					..... Index			cm
Unprimed									
4	7.1	99 a	99 a	99 a	97 ab	16 ab	845 a	802 a	4.01 a
5	6.75	98 a	98 a	98 a	98 a	17 a	809 ab	780 ab	3.8 ab
7	6.4	86 b	86 b	86 b	92 bc	15 bc	768 b	742 b	3.44 c
8	6	88 b	88 b	88 b	89 c	15 c	785 b	744 b	3.65 bc
9	5.9	87 b	87 b	84 b	89 c	14 c	763 b	752 b	3.59 bc
CV	.	3.54	3.54	4.34	4.11	5.03	6.04	5.22	6.13
Dry hydroprimed									
4	6.22	96 ab	96 ab	49 c	100 a	15 ab	811 ab	771 a	3.8 ab
5	7.2	98 a	98 a	56 bc	99 a	16 a	852 a	774 a	4.06 a
7	7.37	85 cd	92 b	66 b	88 b	14 bc	749 b	708 b	3.49 b
8	5.94	91 bc	95 ab	85 a	87 b	14 bc	652 c	713 b	2.75 c
9	5.66	84 d	94 ab	62 bc	90 b	13 c	601 c	702 b	2.49 c
CV	.	4.23	3.38	14.92	2.45	4.07	12.08	6.6	15.7
Hydroprimed stored									
4	7.24	98 a	98 a	25 d	83 b	12 b	724 b	748 b	3.23 ab
5	3.36	98 a	98 a	31 c	97 a	15 a	772 ab	798 a	3.49 a
7	5.29	84 bc	84 bc	49 b	91 a	14 a	729 b	775 ab	2.93 bc
8	5.76	88 b	88 b	70 a	91 a	14 a	785 a	813 a	3.19 ab
9	7.55	81 c	81 c	29 cd	95 a	14 a	665 c	732 b	2.79 c
CV	.	3.85	3.85	10.01	5.39	6.22	7.01	6.2	11.49

Means sharing the same letter do not differ significantly according to the LSD test ($p \leq 0.05$)

The germination performance and vigor tests conducted with the same seeds demonstrated the effectiveness of the methodology based on robust machine learning algorithms in predicting seed performance, as illustrated by the germination test results (*Table 3*). Note that the first canonical correlation R is 0.96 and 0.99 for the Roxa and Vanda genotypes, respectively, corresponding to the correlation between the first pair of canonical variables, L (1). The R^2 values of 0.91 and 0.99 indicate that 91% of the data variability is explained by this correlation for the Roxa genotype and 98% for the Vanda. The test for the hypothesis that the first canonical correlation and all the remaining ones are equal to zero in the population is based on the Lambda statistic with 9 degrees of freedom. In this experiment, the value of the statistic is associated with a 'p' value less than 0.001. Therefore, the first canonical correlation between the machine learning methodology and the seed germination performance tests was significantly different. The second canonical correlation, R= 0.89 (Roxa) and 0.95 (Vanda), and the smaller correlations were not significantly different from zero, as can be seen from the other 'p' values in Table 3. Therefore, one canonical correlation would be sufficient to measure the association between both types of seed analysis methodologies used here. However, it is crucial to emphasize that the impact of hydropriming on seed performance was variable, both for dry hydroprimed seeds and hydroprimed stored seeds, which allowed for vigor classification at different levels. When seeds are hydroprimed, enzyme activity is affected, and the internal structure of protein molecules is disrupted (Farooq et al., 2021). As a seed treatment, it generates noticeable effects on the subsequent development of seedlings (Karaman et al., 2021). This not only impacts seed germination but also leads to

differences in their spectral reflectance, and these differences provide the possibility of identifying the physiological potential of the seeds (Xu et al., 2022).

Table 3. Canonical correlations between seed analysis methodologies based on spectral image values in the bands 388.74 and 1005.98 nm, and lettuce seed vigor tests including moisture content (MC), first germination count (FGC), germination (G), germination after accelerated aging with NaCl saturated solution (AA), seedling emergence (SE), seedling emergence rate index (SEI), vigor index (VI), uniformity index (UI), and average seedling length (Length) obtained by SVIS® for unprimed, dry hydroprimed, and hydroprimed stored seeds

Roxa		
	L (1)	L (2)
R	0.96	0.89
R^2	0.91	0.79
Lambda	32.09	12.57
df	18	8
p-value	0.02	0.13
Vanda		
	L (1)	L (2)
R	0.99	0.95
R^2	0.99	0.91
Lambda	53.03	19.39
df	18	8
p-value	0.02	0.01

Hydropriming has been shown to significantly influence the hyperspectral attributes of lettuce seeds, as evidenced by the results of spectral analysis. The treatments applied resulted in notable differences in spectral bands, with varying impacts on different lettuce genotypes. This variation highlights the importance of considering the response to hydropriming independently for each seed genotype, as emphasized by different authors (Feng et al., 2019; Huang et al., 2016; Wu and Sun, 2013). Furthermore, the analysis of variance (ANOVA) and multivariate analysis of variance (MANOVA) revealed distinct response patterns among genotypes and seed treatments, demonstrating a significant interaction between these factors. These findings are consistent with previous research that underscores the importance of genotype × treatment interaction in determining the hyperspectral properties of seeds (Jones et al., 2018), reinforcing the need for a comprehensive approach in evaluating lettuce seed quality for classification purposes, including variables of interest in seed production programs.

One of the significant contributions of this research is the identification of spectral bands that can be useful in predicting the physiological state of seeds and in developing non-destructive classification techniques. Our data support existing literature on the use of hyperspectral imaging in seed technology (Alves et al., 2023; Cheng et al., 2023; He et al., 2019; Huang et al., 2016). Experimental results, covering different spectral bands, demonstrate that our analysis performs favorably in selecting spectral bands, consistent with other studies. This analytical approach offers advantages over other data preprocessing algorithms, such as PCA, which showed lower sensitivity to outliers, that is, extreme values that could distort the results (Cheng et al., 2023; J. Xia et al., 2016). In this context, the study by Alves et al. (2023) enabled the extraction of features and dimensionality reduction for the selection of important bands in seed classification (28 best-ranked bands out of the 281 bands), which facilitates the application of other machine learning models.

The results from seed germination and vigor tests, compared with machine learning algorithms, showed the utility of spectral bands in seed classification, especially those associated with moisture content. The Random Forest algorithm highlighted the importance of certain spectral bands, such as those in the range of 384 to 390 nm, in predicting differences in seed spectral characteristics and their relationship with germination. These bands emerged as essential predictors, underscoring the utility of hyperspectral imaging in the detailed characterization of seed properties across different genotypes.

The integration of Random Forest and SMOTE resulted in significant improvements in specificity, precision, and sensitivity of the algorithm, making it more robust and reliable in handling imbalanced datasets, as common in data analyses integrating different factors. This combination of hyperspectral imaging techniques with predictive algorithms has shown promising results in predicting seed performance under various conditions. Thus, the integration of hyperspectral imaging techniques with advanced machine learning algorithms validated with seed germination and vigor performance tests offers new perspectives for evaluating and pre-selecting high-quality lettuce seeds based on physiological differences. We invite researchers to enhance the predictive power of the algorithm-based methodology by including new observations and parameters for future research applications.

4. Conclusions

This research demonstrated that hydropriming significantly affects the spectral properties of lettuce seeds, with genotype-dependent variations observed between Roxa and Vanda. The integration of hyperspectral imaging with machine learning algorithms, including Random Forest and SMOTE, facilitated the identification of critical spectral bands linked to physiological performance, notably within the 384.7–390 nm range (região ultravioleta, UV-C). This approach proved to be effective, precise, and non-destructive for seed classification in terms of quality and vigor, presenting a promising tool for seed evaluation and selection in breeding and production programs.

Acknowledgment

To the ‘Doctorado Exterior’ - 885 program of the ‘Ministerio de Ciencia Tecnología e Innovación (MINCIENCIAS) / Colfuturo’, Colombia for the scholarship since 2021.

To the PRO-EX program of Coordenação de Aperfeiçoamento de Pessoal de Nível Superior (CAPES PROEX), Brazil for the scholarship since the beginning of the doctoral program.

Ethical Statement

There is no need to obtain permission from the ethics committee for this study.

Conflicts of Interest

We declare that there is no conflict of interest between us as the article authors.

Authorship Contribution Statement

Concept: Trujillo, H. A., Alves, R. M.; Design: Trujillo, H. A., Alves, R. M., Gomes-Junior, G. M.; Data Collection or Processing: Trujillo, H. A., Iost-Filho, F. H., Velasquez-Vasconez, P. A.; Statistical Analyses: Velasquez-Vasconez, P. A., Trujillo, H. A.; Literature Search: Trujillo, H. A.; Writing, Review and Editing: Trujillo, H. A., Alves, R. M., Gomes-Junior, G. M., Velasquez-Vasconez, P. A., Iost-Filho, F. H.

References

Alhamdan, A. M. and Atia, A. (2017). Non-destructive method to predict Barhi dates quality at different stages of maturity utilizing near-infrared (NIR) spectroscopy. *International Journal of Food Properties*, 20(3): 2950–2959.

Ali, A., Machado, V. S. and Hamill, A. S. (1990). Osmoconditioning of tomato and onion seeds. *Scientia Horticulturae*, 43(3–4): 213–224.

Alves, R. M., Gomes-Junior, F. G., Carmo-Filho, A. d. S., Ribeiro, G. d. F. R., Rego, C. H. Q., Iost-Filho, F. H. and Yamamoto, P. T. (2023). Evaluation of the effect of the vigor of soybean seeds treated with micronutrients using X-ray fluorescence spectroscopy and hyperspectral imaging. *Agronomy*, (13): 1945.

Arngren, M., Hansen, P. W., Eriksen, B., Larsen, J. and Larsen, R. (2011). Analysis of pregerminated barley using hyperspectral image analysis. *Journal of Agricultural and Food Chemistry*, 59(21): 11385–11394.

Bai, R., Zhou, J., Wang, S., Zhang, Y., Nan, T., Yang, B., Zhang, C. and Yang, J. (2024). Identification and classification of coix seed storage years based on hyperspectral imaging technology combined with deep learning. *Foods*, 13(3): 498.

Beyaz, R. (2023). Germination and seedling properties of *Lotus corniculatus* (L.) under simulated drought stress. *Journal of Tekirdag Agricultural Faculty,* 20(4): 879–889. (In Turkish)

Brasil (2009). Rules for Seed Testing. Ministry of Agriculture, Livestock and Food Supply (MAPA), Brasília, Brazil. (In Portuguese)

Bruggink, G.T., Ooms, J. J. J. and van der Toorn, P. (1999). Induction of longevity in primed seeds. *Seed Science Research*, 9(1): 49–53.

Cheng, T., Chen, G., Wang, Z., Hu, R., She, B., Pan, Z., Zhou, X. G., Zhang, G. and Zhang, D. (2023). Hyperspectral and imagery integrated analysis for vegetable seed vigor detection. *Infrared Physics and Technology*, 131: 104605.

Choi, J. Y., Heo, S., Bae, S., Kim, J. and Moon, K. D. (2020). Discriminating the origin of basil seeds (*Ocimum basilicum* (L.)) using hyperspectral imaging analysis. *LWT - Food Science and Technology*, 118: 108715.

Christensen, R. H. B. (2023). Ordinal Regression Models for Ordinal Data. R Package Version 2023, 12-4.

Dale, L. M., Thewis, A., Boudry, C., Rotar, I., Dardenne, P., Baeten, V. and Pierna, J. A. F. (2013). Hyperspectral imaging applications in agriculture and agro-food product quality and safety control: A review. *Applied Spectroscopy Reviews*, 48(2): 142–159.

Farooq, M., Basra, S. M. A., Afzal, I. and Khaliq, A. (2006). Optimization of hydropriming techniques for rice seed invigoration. *Seed Science and Technology*, 34(2): 507–512.

Farooq, M., Romdhane, L., Rehman, A., Al-Alawi, A. K. M., Al-Busaidi, W. M., Asad, S. A. and Lee, D. J. (2021). Integration of seed priming and biochar application improves drought tolerance in cowpea. *Journal of Plant Growth Regulation*, 40(5): 1972–1980.

Feng, L., Zhu, S., Liu, F., He, Y., Bao, Y. and Zhang, C. (2019). Hyperspectral imaging for seed quality and safety inspection: A review. *Plant Methods*, 15(1): 91.

Feng, X., Zhao, Y., Zhang, C., Cheng, P. and He, Y. (2017). Discrimination of transgenic maize kernel using NIR hyperspectral imaging and multivariate data analysis. *Sensors*, 17(8): 1894.

Ge, Y., Song, S., Yu, S., Zhang, X. and Li, X. (2024). Rice seed classification by hyperspectral imaging system: A real-world dataset and a credible algorithm. *Computers and Electronics in Agriculture*, 219: 108776.

Guo, D., Zhu, Q., Huang, M., Guo, Y. and Qin, J. (2017). Model updating for the classification of different varieties of maize seeds from different years by hyperspectral imaging coupled with a pre-labeling method. *Computers and Electronics in Agriculture*, 142: 1–8.

He, X., Feng, X., Sun, D., Liu, F., Bao, Y. and He, Y. (2019). Rapid and nondestructive measurement of rice seed vitality of different years using near-infrared hyperspectral imaging. *Molecules*, 24(12): 2227.

Huang, M., Tang, J., Yang, B. and Zhu, Q. (2016). Classification of maize seeds of different years based on hyperspectral imaging and model updating. *Computers and Electronics in Agriculture*, 122: 139–145.

Ibrahim, E. A. (2016). Seed priming to alleviate salinity stress in germinating seeds. *Journal of Plant Physiology*, 192: 38–46.

Iost Filho, F. H., de Bastos, J., de Medeiros, A. D., Rosalen, D. L. and Yamamoto, P. T. (2022). Assessment of injury by four major pests in soybean plants using hyperspectral proximal imaging. *Agronomy*, 12(7): 1516.

Karaman, R., Türkay, C. and Akgün, İ. (2021). Effects of oat grass juice on germination and seedling characteristics of certain weeds and cultivated plants. *Journal of Tekirdag Agricultural Faculty,* 18(2): 312–321. (In Turkish)

Kikuti, A. L. P. and Marcos-Filho, J. (2012). Vigor tests in lettuce seeds. *Horticultura Brasileira*, 30(1): 44–50. (In Portuguese)

Krepper, G., Romeo, F., Fernandes, D. D. de S., Diniz, P. H. G. D., de Araújo, M. C. U., di Nezio, M. S., Pistonesi, M. F. and Centurión, M. E. (2018). Determination of fat content in chicken hamburgers using NIR spectroscopy and the successive projections algorithm for interval selection in PLS regression (iSPA-PLS). *Spectrochimica Acta Part A: Molecular and Biomolecular Spectroscopy*, 189: 300–306.

Liu, Y., Xie, H., Chen, Y., Tan, K., Wang, L. and Xie, W. (2016). Neighborhood mutual information and its application on hyperspectral band selection for classification. *Chemometrics and Intelligent Laboratory Systems*, 157: 140–151.

Loewe, V., Navarro, C. R. M., García, O. J., Riccioli, C. and Sánchez, C. R. (2017). discriminant analysis of Mediterranean pine nuts (*Pinus pinea* (L.)) from Chilean plantations by near infrared spectroscopy (NIRS). *Food Control*, 73: 634–643.

Nicolaï, B. M., Beullens, K., Bobelyn, E., Peirs, A., Saeys, W., Theron, K. I. and Lammertyn, J. (2007). Nondestructive measurement of fruit and vegetable quality by means of NIR spectroscopy: A review. *Postharvest Biology and Technology*, 46(2): 99–118.

Parmley, K., Nagasubramanian, K., Sarkar, S., Ganapathysubramanian, B. and Singh, A. K. (2019). Development of optimized phenomic predictors for efficient plant breeding decisions using phenomic-assisted selection in soybean. *Plant Phenomics*, 2019:5809404.

Qiu, C., Ding, F., He, X. and Wang, M. (2023). Apply physical system model and computer algorithm to identify *Osmanthus fragrans* seed vigor based on hyperspectral imaging and convolutional neural network. *Information Technology and Control*, 52(4): 887–897.

Raj, A. B. and Raj, S. K. (2019). Seed priming: An approach towards agricultural sustainability. *Journal of Applied and Natural Science*, 11(1): 227–234.

R Core Team. (2023). R: A Language and Environment for Statistical Computing. R Foundation for Statistical Computing, Vienna, Austria.

Sako, Y., McDonald, M. B., Fujimura, K., Evans, A. F. and Bennett, Mark. (2001). A system for automated seed vigor assessment. *Seed Science and Technology*, 29: 625–636.

Singh, C. B., Jayas, D. S., Paliwal, J. and White, N. D. G. (2009). Detection of sprouted and midge-damaged wheat kernels using near-infrared hyperspectral imaging. *Cereal Chemistry*, 86(3): 256–260.

Sun, J., Jiang, S., Mao, H., Wu, X. and Li, Q. (2016). Classification of black beans using visible and near infrared hyperspectral imaging. *International Journal of Food Properties*, 19(8): 1687–1695.

Wang, C., Liu, B., Liu, L., Zhu, Y., Hou, J., Liu, P. and Li, X. (2021). A review of deep learning used in the hyperspectral image analysis for agriculture. *Artificial Intelligence Review*, 54(7): 5205–5253.

Wu, D. and Sun, D. W. (2013). Advanced applications of hyperspectral imaging technology for food quality and safety analysis and assessment: A review — Part I: Fundamentals. *Innovative Food Science and Emerging Technologies*, 19: 1–14.

Xia, J., Chanussot, J., Du, P. and He, X. (2016). Rotation-based support vector machine ensemble in classification of hyperspectral data with limited training samples. *IEEE Transactions on Geoscience and Remote Sensing*, 54(3): 1519–1531.

Xia, Y., Xu, Y., Li, J., Zhang, C. and Fan, S. (2019). Recent advances in emerging techniques for non-destructive detection of seed viability: A review. *Artificial Intelligence in Agriculture*, 1: 35–47.

Xing, J., Symons, S., Shahin, M. and Hatcher, D. (2010). Detection of sprout damage in Canada Western Red Spring wheat with multiple wavebands using visible/near-infrared hyperspectral imaging. *Biosystems Engineering*, 106(2): 188–194.

Xu, Y., Wu, W., Chen, Y., Zhang, T., Tu, K., Hao, Y., Cao, H., Dong, X. and Sun, Q. (2022). Hyperspectral imaging with machine learning for non-destructive classification of *Astragalus membranaceus* var. *mongholicus*, *Astragalus membranaceus*, and similar seeds. *Frontiers in Plant Science*, 13: 1031849.

Yin, H., Xie, B., Chen, B., Ma, J., Chen, J., Zhou, Y., Han, X., Xiong, Z., Yu, Z. and Huang, F. (2023). Detection of moisture content and size of pumpkin seeds based on hyperspectral reflection and transmission imaging techniques. *Journal of Food Composition and Analysis*, 124: 105651.

Yin, W., Zhang, C., Zhu, H., Zhao, Y. and He, Y. (2017). Application of near-infrared hyperspectral imaging to discriminate different geographical origins of Chinese wolfberries. *Plos One*, 12(7): e0180534.

Zhang, B., Huang, W., Li, J., Zhao, C., Fan, S., Wu, J. and Liu, C. (2014). Principles, developments and applications of computer vision for external quality inspection of fruits and vegetables: A review. *Food Research International*, 62: 326–343.

Zhang, L., Sun, H., Rao, Z. and Ji, H. (2020). Hyperspectral imaging technology combined with deep forest model to identify frost-damaged rice seeds. *Spectrochimica Acta Part A: Molecular and Biomolecular Spectroscopy*, 229: 117973.

Zhao, Y., Zhang, C., Zhu, S., Gao, P., Feng, L. and He, Y. (2018). Non-destructive and rapid variety discrimination and visualization of single grape seed using near-infrared hyperspectral imaging technique and multivariate analysis. *Molecules*, 23(6): 1352.

Zou, Z., Chen, J., Zhou, M., Zhao, Y., Long, T., Wu, Q. and Xu, L. (2022). Prediction of peanut seed vigor based on hyperspectral images. *Food Science and Technology*, 42: e32822.